

Combining Probes

Anaïs Rassat¹, François Lanusse, Donnacha Kirk, Ole Host
and Sarah Bridle

¹Laboratory of Astrophysics, Ecole Polytechnique Fédérale de Lausanne (EPFL)
email: anaïs.rassat@epfl.ch

Abstract. With the advent of wide-field surveys, cosmology has entered a new golden age of data where our cosmological model and the nature of dark universe will be tested with unprecedented accuracy, so that we can strive for high precision cosmology. Observational probes like weak lensing, galaxy surveys and the cosmic microwave background as well as other observations will all contribute to these advances. These different probes trace the underlying expansion history and growth of structure in complementary ways and can be combined in order to extract cosmological parameters as best as possible. With future wide-field surveys, observational overlap means these will trace the same physical underlying dark matter distribution, and extra care must be taken when combining information from different probes. Consideration of probe combination is a fundamental aspect of cosmostatistics and important to ensure optimal use of future wide-field surveys.

Keywords. cosmology, methods: statistics

1. Introduction

In recent decades, complementary observational cosmological probes have contributed to building our currently accepted standard model of cosmology: a universe dominated by a mysterious dark energy required to explain its acceleration and with most matter being in the form of yet another mysterious component called dark matter. The matter-energy densities (Ω_{DE} , Ω_{DM} , etc . . .) have been studied quantitatively for several decades, often referred to as “precision cosmology” (Dicke *et al.* (1965)). However, this picture of our Universe leaves room for several open questions: 1) on the nature of dark energy and 2) the nature of dark matter, 3) on understanding the initial conditions of the Universe and 4) on testing whether Einstein’s theory of General Relativity is the correct prescription for gravity on cosmological scales. Answering these questions requires new physical parameters to be considered.

To answer these open questions, cosmologists have access to two fundamental probes: the expansion history of the Universe and the growth of structures. In practice, these can be observed through several observational probes. At low redshifts, weak gravitational lensing, galaxy clustering (Albrecht *et al.* (2006), Peacock *et al.* (2006)), as well as strong lensing and other observables have been used and are promising tools for further experiments. At high redshift, the cosmic microwave background has been studied extensively with COBE (Bennett *et al.* (1990)), WMAP (Bennett *et al.* (2013)) and Planck (Planck Collaboration (2011)) as well as other smaller scale experiments. Cross-correlation of low and high redshift observables have also been used to further constrain our cosmological model, as for example with the integrated Sachs-Wolfe (ISW) effect (Sachs & Wolfe (1967)).

With the advent of wide-field surveys, observational overlap means that different observational probes will trace the same physical underlying dark matter distribution and

extra care must be taken when combining information. This consideration of probe combination methods is a fundamental aspect of reaching precision and accurate cosmology.

2. Forecasting with the Fisher Information Matrix

In order to discuss the constraining power of different observational probes and how best to combine them, we consider the Fisher Information Matrix (FIM).

2.1. Fisher Information Matrix (FIM)

It is possible to forecast the precision with which a future experiment will be able to constrain cosmological parameters, by using the FIM (for a detailed derivation of the following see Tegmark *et al.* (1997) or Dodelson (2003)). This method requires only three fundamental ingredients:

- A set of cosmological parameters $\vec{\theta}$ for which one wants to forecast errors, and assumed values of these for a true underlying universe. For example, this could be a set of parameters $\vec{\theta} = (\Omega_{DE}, w_0)$ for which one can assume: $\Omega_{DE}^{true} = 0.75, w_0^{true} = -1$.
- A set of n measurements of the data $\vec{x} = (x_1, x_2, \dots, x_n)$, say the gravitational weak lensing angular power spectrum $C_{GG}(\ell)$ over a range $\ell = 1 \dots n$, and a model for how the data depend on cosmological parameters, i.e.: $C_{GG}(\ell) = C_{GG}(\ell, \vec{\theta})$
- An estimate of the uncertainty on the data $\Delta C_{GG}(\ell)$, which may depend on the given experiment (instrument noise, shot noise, etc...) as well on the data estimator (e.g., cosmic variance).

The FIM is defined by:

$$F_{\alpha\beta} = \left\langle \frac{\partial^2 \mathcal{L}}{\partial \theta_\alpha \partial \theta_\beta} \right\rangle, \tag{2.1}$$

where $\mathcal{L} = -\ln L$ and $L = L(\vec{x}, \vec{\theta})$ is the likelihood function or the probability distribution of the data \vec{x} , which depends on some model parameter set $\vec{\theta}$. If the data are correlated, the Fisher matrix then this might instead be the inverse of the covariance matrix between data points. In this chapter, I only consider uncorrelated data points.

The uncertainty on the parameter θ_α can be estimated directly from the FIM and has been shown to obey:

$$\Delta\theta_\alpha \geq \frac{1}{\sqrt{F_{\alpha\alpha}}}, \tag{2.2}$$

if all other parameters are known. This is known as the Cramér-Rao inequality. This is the key strength of the FIM forecast method, in that it places a solid lower limit on the parameter uncertainties, if the underlying probability distribution $L(\vec{x}, \vec{\theta})$ is Gaussian. If the parameters $\vec{\theta}$ also have Gaussian distribution around the fiducial value, then:

$$\Delta\theta_\alpha = \frac{1}{\sqrt{F_{\alpha\alpha}}}, \tag{2.3}$$

when all the other parameters are fixed.

If the vector of parameters $\vec{\theta}$ is allowed to vary, then the uncertainties for each parameter can still be obtained, and obey:

$$\Delta\theta_\alpha \geq \sqrt{(F^{-1})_{\alpha\alpha}}, \tag{2.4}$$

where F^{-1} is the inverse of the FIM. In this case, the uncertainty for θ_α has been obtained by implicitly marginalising over the other parameters. An unmarginalised estimate of the uncertainty of θ_α would be $1/\sqrt{F_{\alpha\alpha}}$.

By assuming the errors on the spherical harmonic estimator $C_{GG}(\ell)$ are Gaussian, then:

$$F = \left\langle \frac{\partial \mathcal{L}}{\partial \theta_\alpha \partial \theta_\beta} \right\rangle = \frac{1}{2} \left\langle \frac{\partial^2 \chi^2}{\partial \theta_\alpha \partial \theta_\beta} \right\rangle, \quad (2.5)$$

since $\mathcal{L} = -\ln L = \frac{1}{2}\chi^2$. Using the definition of χ^2 :

$$F_{\alpha\beta} \simeq \sum_{\ell} \frac{1}{(\Delta C_{GG})^2} \frac{\partial C_{GG}}{\partial \theta_\alpha} \frac{\partial C_{GG}}{\partial \theta_\beta}, \quad (2.6)$$

where C_{GG} implicitly depends on ℓ and there is no covariance between the data points.

2.2. Figure of Merits (FoM)

In the context of future wide-field survey optimisation, it is often useful to have a single quantity or *Figure of Merit (FoM)* in order to compare the constraining power of different surveys or survey configurations. If one is interested in dark energy parameters, one can use the dark energy FoM:

$$\text{FoM}_{\text{DE}} = \frac{1}{\sigma_{w_0} \sigma_{w_p}}, \quad (2.7)$$

where σ_{w_0} and σ_{w_p} are the marginalised errors, and w_p is the dark energy equation of state parameter at the pivot redshift.

In order to compare the constraining power across different sectors of the cosmological model, one can use a more general FoM which encompasses information from several cosmological parameters, i.e. :

$$\text{FoM}_{\text{TOT}} \equiv \ln \left(\frac{1}{\det (F^{-1})_{\text{cosm}}} \right). \quad (2.8)$$

3. Observables vs. Probes

3.1. Distinction between an observable and a probe

It is useful to state the distinction here between an *observable* and a *probe*, with a probe relating to a physical effect and an observable being independent of any model. Often different probes are folded into a single observables, and different observables can fundamentally measure a single probe. As an example, different observables are:

- ϵ : galaxy ellipticities,
- n : galaxy number counts,
- T : temperature.

Each observable can contain information related to several probes, e.g.:

- ϵ : gravitational lensing and intrinsic alignments,
- n : galaxy clustering (including redshift distortions, baryon acoustic oscillations) and cosmic magnification,
- T : primary and secondary temperature fluctuations in the CMB.

Here, we give a few examples of how probe combination within a single observable can have an important impact on observational cosmology or be useful to constrain different sectors of the cosmological model.

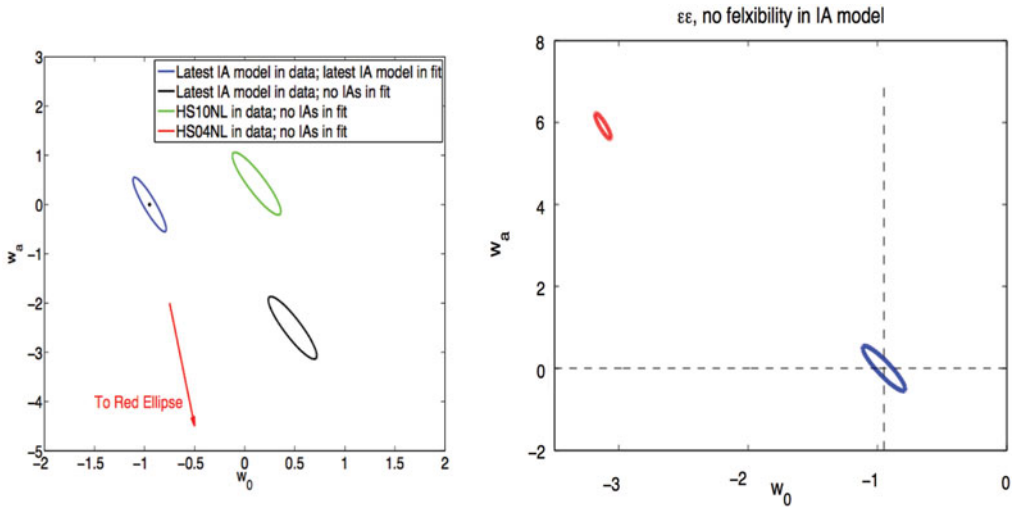


Figure 1. Taken from Kirk *et al.* (2012). *Left:* this figure shows the effect of ignoring intrinsic alignments for different physical models by showing the cosmological bias on dark energy parameters w_0 and w_a (95% confidence limits). *Right:* This figure shows the effect of using the 'wrong' IA model on cosmological parameters. In blue the latest IA model is used in the data and in the fit, whereas in red, the latest IA model is in the data but an older IA model is used in the fit.

3.2. Intrinsic alignments and galaxy ellipticities

Weak gravitational lensing has been shown to be one of the most promising probes to study the nature of dark energy. Gravitational lensing can be studied statistically by looking at the correlation function of galaxy ellipticities. One fundamental assumption is that galaxies are randomly oriented before they are affected by gravitational lensing. However, it is known that galaxies can have intrinsic alignments due to tidal forces so that the measured ellipticity is statistically given by:

$$\epsilon = \gamma + I, \tag{3.1}$$

where γ is the galaxy shear and I is the intrinsic alignment component so that the total measured correlation function is given by (for references and further details, see Kirk *et al.* (2012):

$$C_{\epsilon\epsilon} = C_{GG} + C_{II} + C_{GI}. \tag{3.2}$$

The IA terms contain cosmological information through their dependence on the matter power spectrum and is therefore a secondary probe that can help constrain cosmology. not only does IA contain extra cosmological information, but ignoring this effect can lead to a bias on cosmological parameters as shown in the left hand side of figure 1 taken from Kirk *et al.* (2012) showing the importance of performing an analysis including secondary signals from the start.

In the right hand side of figure 1, also taken from Kirk *et al.* (2012), shows the cosmological bias from a different IA model in the analysis than the one contained in the observable, showing again the importance of a good physical model for secondary probes.

3.3. Galaxy number counts

Galaxy number counts are used in the literature to measure clustering information in the large scale structure (LSS) by indirectly measure the matter power spectrum. As shown in figure 2, the matter power spectrum itself measures different physical effects or

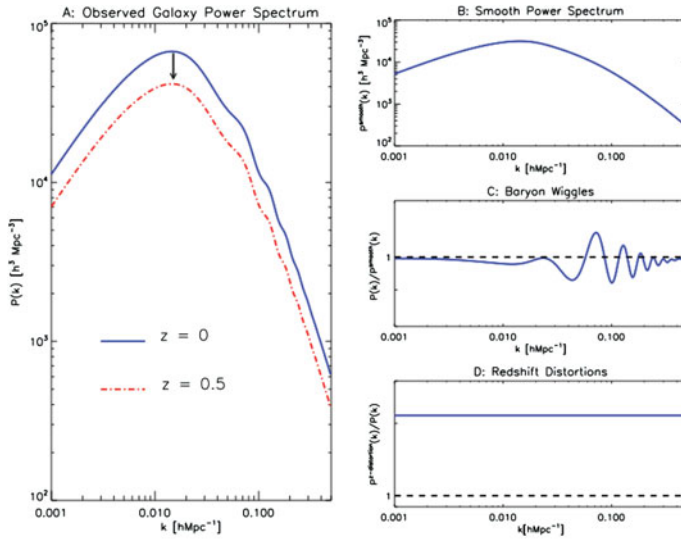


Figure 2. Taken from Rassat *et al.*(2008). The matter power spectrum is shown on the left, and different physical components or probes are shown on the right, including: the broad band power spectrum, baryon acoustic oscillations and redshift distortions.

probes, for e.g.: the broad band power spectrum, baryon acoustic oscillations and redshift distortions. Each of which probe cosmological parameters in different and complementary ways.

4. Probe Combination: Cross-correlations as a probe

Previously, we have briefly discussed how different observables can be studied by considering their auto-correlation functions. Cross-correlating different observables can also be used to study certain physical effects that are different to study with the auto-correlations, such as the integrated Sachs-Wolfe effect, which we discuss in section 4.1. We also use the example of tomographic analysis of LSS to show the importance of using cross-correlations in section 4.2.

4.1. The integrated Sachs-Wolfe effect

As photons from the last scattering surface travel towards us, they pass through the gravitational potentials of structures along the line of sight. Photons will gain energy as they enter the gravitational potentials and lose energy on exit. If the potential is unchanged during this travel time, the net effect will be null. However, if the gravitational potential decreases with time (as in universes with dark energy, positive curvature or in some alternative models), the net effect will be that photons will have gained energy by passing through the gravitational potentials. This effect, called the integrated Sachs-Wolfe effect, adds power to the observed CMB temperature-temperature power spectrum, but is difficult to measure due to cosmic variance. Instead, this effect can be measured by cross-correlating tracers of the gravitational potential (e.g. with galaxy surveys) with the CMB (Sachs & Wolfe (1967), Boughn & Crittenden(2002), Rassat *et al.* (2007)).

Measuring the ISW effect can be used as an independent measure of the presence of dark energy, as well as a measure of its equation of state parameters. Though the effect is small, combination of different tracers of large scale structure at different redshifts can also increase the amplitude of the signal (Giannantonio *et al.* (2008)).

Reconstructing the ISW effect (Dupé *et al.* (2011), Rassat & Starck (2013), Rassat *et al.* (2013)Rassat, Starck, & Dupe, Rassat *et al.* (2014)), i.e. by reconstructing a map of the temperature anisotropies due to the ISW effect can be used to study claimed anomalies in the anisotropies of the primordial CMB. The premise is that the most interesting cause of the anomalies would be one resulting from early Universe physics, and that we are therefore interested in studying the primordial CMB instead of the observed CMB, i.e., one free from Galactic emissions, astrophysical and secondary cosmological foregrounds. The observed CMB temperature fluctuations can be written as:

$$\delta_T^{\text{OBS}} = \delta_T^{\text{prim}} + \delta_T^{\text{ISW}} + \delta_T^{\text{other}} + \delta_T^{\mathcal{N}}, \quad (4.1)$$

where δ_T^{OBS} is the total observed CMB, δ_T^{prim} the primordial CMB fluctuations, δ_T^{ISW} the signal due to the ISW effect, δ_T^{other} other effects, and $\delta_T^{\mathcal{N}}$ the noise. On large scales, δ_T^{other} is expected to include the kinetic Sunyaev-Zel'dovich and the kinetic Doppler quadrupole effects, and $\delta_T^{\mathcal{N}}$ should be negligible.

Recently, Rassat *et al.* (2014) analysed six of these claimed anomalies in a new full-sky map of the CMB (provided in Bobin *et al.* (2013)). Analysis of the observed CMB maps showed that only the low quadrupole and quadrupole-octopole alignment seemed significant, but that the planar octopole, Axis of Evil, mirror parity and cold spot were not significant. After subtraction of astrophysical (kinetic Sunyaev-Zel'dovich) and cosmological secondary effects (ISW and the kinetic Doppler quadrupole), only the low quadrupole could still be considered anomalous, meaning the significance of only one anomaly was affected by secondary effect subtraction out of six anomalies considered.

4.2. Large Scale Structure: tomography vs. 3D analysis

Unlike the CMB, information in a spectroscopic galaxy survey will be 3-dimensional. It can therefore naturally be split into radial bins. Cosmological information is contained in each bin, but also in the cross-correlation between redshift bins. The question is therefore of how best to combine the information from the galaxy number counts to extract the 3-dimensional information.

This can be done either using tomography, i.e. a spherical harmonic approach including cross-correlation between various bins, or using a full 3D spherical Fourier-Bessel (SFB) approach (Heavens & Taylor (1995)), i.e. by decomposing the field using:

$$f(\vec{r}) = \sqrt{\frac{2}{\pi}} \int dk \sum_{\ell m} f_{\ell m}(k) k j_{\ell}(k r) Y_{\ell m}(\theta, \phi). \quad (4.2)$$

The SFB approach is motivated physically and has natural prescription for selection and physical effects (e.g., redshift distortions).

Figure 3 is taken from Lanusse *et al.* (2014) and shows that while a tomographic reconstruction can recover the information extracted using a SFB analysis, in the case where nuisance parameters are included, the 3D approach should be preferred (see Lanusse *et al.* (2014) for details).

5. Probe Combination: Uncorrelated probes and priors

Different observables can constrain cosmological parameters in complementary ways, for e.g. by having different directions of degeneracy. This complementarity can be used to provide higher precision constraints. For independent probes A and B, the forecasting FIMs can simply be added so that:

$$F_{\text{TOT}} = F_A + F_B. \quad (5.1)$$

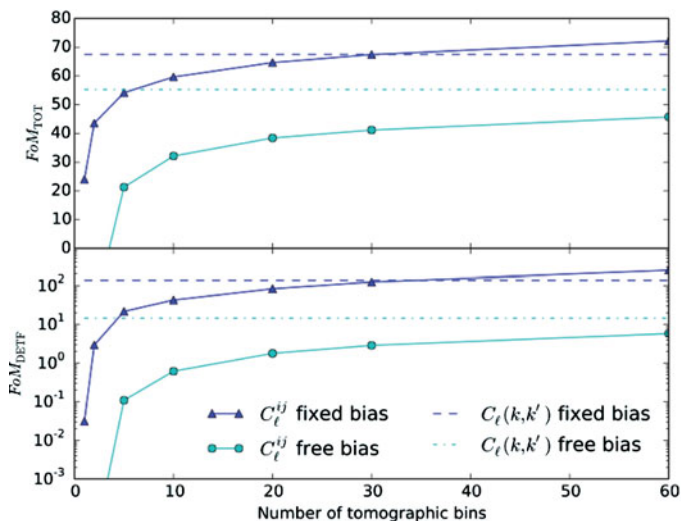


Figure 3. Taken from Lanusse *et al.* (2014). The two different figures of merit for a tomographic vs. SFB analysis, considering only cosmological parameters (top) or including nuisance parameters (bottom).

This method can be applied to different observables of a same experiment (e.g., the expected constraints from gravitational lensing and galaxy number counts for a given wide-field survey), as well as for constraints from different experiments, or to include priors from past experiments.

Combining information in such a way can be used to either provide tighter constraints on cosmological parameters, or expand the parameter space to include more general parameters. For example, by including CMB Planck priors with gravitational lensing constraints, one can expand the parameters space of the initial conditions sector whilst simultaneously allowing for massive neutrinos (Debono *et al.* (2009)). The parameter space can also be expanded to simultaneously constrain dark energy and modified gravity parameters (Laureijs *et al.* (2011)).

6. Probe Combination: Accounting for correlations

For future wide-field surveys, observational overlap will mean that different observables will often probe the same physical underlying dark matter field, so that these will not in practice be uncorrelated observables. Taking the example of galaxy ellipticities ϵ and galaxy number counts n as before. In section 5, we considered the observables $C_{\epsilon\epsilon}$ and C_{nn} separately. If the observables are correlated, we must consider the $C_{n\epsilon}$ as a new measurement. In this case, we can no longer consider the Fisher matrices to simply add as in equation 5.1, but must calculate a single Fisher matrix for all observables using a covariance matrix which takes into account correlations. The Fisher matrix elements are given by (see Joachimi & Bridle (2010) for full details):

$$F_{\alpha\beta} = \sum_{l=l_{min}}^{l_{max}} \sum_{(i,j),(m,n)} \frac{\partial C_{ij}(l)}{\partial \theta_\alpha} \text{Cov}^{-1} [C_{ij}(l), C_{mn}(l)] \frac{\partial C_{mn}(l)}{\partial \theta_\beta}. \tag{6.1}$$

Where the power spectra are now combined into a total data vector:

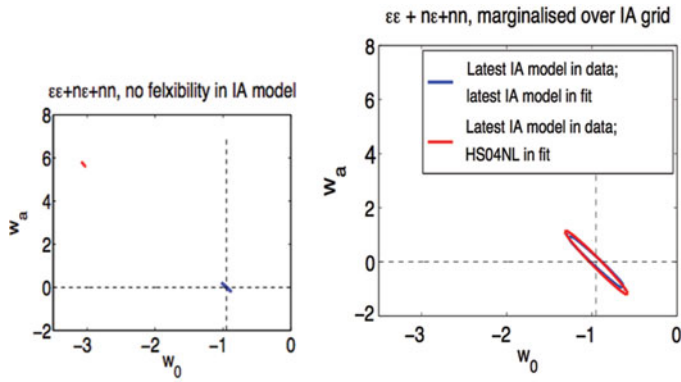


Figure 4. Taken from Kirk *et al.* (2012). The 95% confidence limits on dark energy parameters w_0 and w_a from galaxy ellipticities and number counts, accounting for correlations between both observables, in the context of a future wide-field survey. The blue contours have the same intrinsic alignment model in the fit as in the data, while the red contours have another intrinsic alignment model in the fit. In the left hand side, the Fisher matrix contains only cosmological parameters, while in the right hand side nuisance parameters regarding the galaxy bias and intrinsic alignment amplitude have been marginalised over. In the case where nuisance parameters are considered, the cosmological bias is not longer problematic.

$$\mathcal{D}(\ell) = \left\{ C_{\epsilon\epsilon}^{(11)}(\ell), \dots, C_{\epsilon\epsilon}^{(N_{z\text{bin}} N_{z\text{bin}})}(\ell), C_{n\epsilon}^{(11)}(\ell), \dots, \right. \tag{6.2}$$

$$\left. C_{n\epsilon}^{(N_{z\text{bin}} N_{z\text{bin}})}(\ell), C_{nn}^{(11)}(\ell), \dots, C_{nn}^{(N_{z\text{bin}} N_{z\text{bin}})}(\ell) \right\}$$

for every angular frequency considered. The corresponding covariance, again for every ℓ , reads

$$\text{Cov}(\ell) = \left(\frac{\begin{array}{ccc} \text{Cov}_{\epsilon\epsilon\epsilon\epsilon}^{(ijkl)}(\ell) & | & \text{Cov}_{\epsilon\epsilon n\epsilon}^{(ijkl)}(\ell) & | & \text{Cov}_{\epsilon\epsilon nn}^{(ijkl)}(\ell) \\ \text{Cov}_{n\epsilon\epsilon\epsilon}^{(ijkl)}(\ell) & | & \text{Cov}_{n\epsilon n\epsilon}^{(ijkl)}(\ell) & | & \text{Cov}_{n\epsilon nn}^{(ijkl)}(\ell) \\ \text{Cov}_{nn\epsilon\epsilon}^{(ijkl)}(\ell) & | & \text{Cov}_{nn n\epsilon}^{(ijkl)}(\ell) & | & \text{Cov}_{nn nn}^{(ijkl)}(\ell) \end{array}}{\quad}, \right) \tag{6.3}$$

where the sub-matrices are the usual matrices for each individual observable (i.e., $C_{\epsilon\epsilon}$, C_{nn} , $C_{n\epsilon}$).

In this approach, different probes are combined in several ways. Several probes are folded directly into single observables (e.g., intrinsic alignments and weak gravitational lensing are both included in the physical effects contributing to galaxy ellipticities), while correlations between different observables are accounted for in the covariance matrix.

This “full” calculation returns tighter constraints than using only information from the galaxy ellipticities (Kirk *et al.* (2013)), as shown in the left-hand side of figure 4. However, there is still evidence of a catastrophic bias on the cosmological parameters when the ‘wrong’ intrinsic alignment model is used to fit the data, indicating that including all secondary signals is still of utmost importance for precision and accurate cosmology even when correlations between galaxy ellipticities and number counts are accounted for. However, in the right hand side of figure 4, the same calculation is done using a series of nuisance parameters (see Kirk *et al.* 2012 for details).

7. Conclusion

The 20th century saw cosmology transition from a theoretical endeavour to data-driven field. With the advent of future wide-field surveys covering large areas on the sky and wide redshift ranges, this new golden age of data in cosmology will no longer be limited by access to data but by statistical challenges in their processing. Observables such as galaxy ellipticities, galaxy number counts and temperature fluctuations in the microwave sky are each linked to a variety of physical effects, sometimes present in different observables. Future surveys are aiming at high precision cosmology, and correct treatment of all of these effects will be necessary to achieve not only precision cosmology but also accurate cosmology.

These observables can also be cross-correlated in order to study subtle physical effects like the integrated Sachs-Wolfe effect. In addition, correct understanding of these different effects can also help link different sectors of the cosmological model, for example, a correct understanding of secondary cosmological effects in the CMB can help recover the primordial CMB temperature fluctuations.

Together these observables will trace the underlying expansion history and growth of structure in complementary ways and can be combined in order to extract cosmological parameters as best as possible. With future wide-field surveys, observational overlap means these will trace the same physical underlying dark matter distribution, and extra care must be taken when combining information from different probes.

Consideration of probe combination is a fundamental aspect of cosmostatistics and important to ensure optimal use of future wide-field surveys. Probe combination will require combining information from different fields and sub-fields of astrophysics, cosmology and statistics, linking specialists working on different observational probes but that might be considering similar or identical effects, meaning effort within the cosmological community may be duplicated. This effort might be made more efficient by a systematic commitment by all researchers to reproducible research, which includes publication of codes and intermediate results both for existing data analysis and future forecasts.

Acknowledgement

This research is in part supported by the Swiss National Science Foundation (SNSF)

References

- Albrecht, A., Bernstein, G., Cahn, R., *et al.* 2006, ArXiv e-prints 0609591
- Bennett, C. L., Larson, D., Weiland, J. L., *et al.* 2013, *ApJS*, 208, 20
- Bennett, C. L., Smoot, G. F., & Kogut, A. 1990, in Bulletin of the American Astronomical Society, Vol. 22, Bulletin of the American Astronomical Society, 1336–+
- Bobin, J., Sureau, F., Paykari, P., *et al.* 2013, *A & A*, 553, L4
- Boughn, S. P. & Crittenden, R. G. 2002, *Physical Review Letters*, 88, 021302
- Debono, I., Rassat, A., Refregier, A., Amara, A., & Kitching, T. D. 2010, *MNRAS*, 404, 110
- Dicke, R. H., Peebles, P. J. E., Roll, P. G., & Wilkinson, D. T. 1965, *ApJ*, 142, 414
- Dodelson, S. 2003, *Modern Cosmology*, Amsterdam (Netherlands): Academic Press. ISBN 0-12-219141-2
- Dupé, F.-X., Rassat, A., Starck, J.-L., & Fadili, M. J. 2011, *Astronomy & Astrophysics*, 534, A51
- Giannantonio, T., Scranton, R., Crittenden, R., *et al.* 2008, *Physical Review D*, 77, 123520
- Heavens, A. F. & Taylor, A. N. 1995, *MNRAS*, 275, 483
- Joachimi, B. & Bridle, S. L. 2010, *A&A*, 523, A1
- Kirk, D., Lahav, O., Bridle, S., *et al.* 2013, ArXiv e-prints 1307.8062
- Kirk, D., Rassat, A., Host, O., & Bridle, S. 2012, *MNRAS*, 424, 1647

- Lanusse, F., Rassat, A., & Starck, J. 2014, ArXiv e-prints 1406.5989
- Laureijs, R., Amiaux, J., Arduini, S., *et al.* 2011, ArXiv e-prints 1110.3193
- Peacock, J. A., Schneider, P., Efstathiou, G., *et al.* 2006, ESA-ESO Working Group on "Fundamental Cosmology", Tech. rep., ArXiv e-prints 0610906
- Planck Collaboration, Ade, P. A. R., Aghanim, N., *et al.* 2011, *A&A*, 536, A1
- Rassat, A., Land, K., Lahav, O., & Abdalla, F. B. 2007, *MNRAS*, 377, 1085
- Rassat, A. & Starck, J.-L. 2013, *A&A*, 557, L1
- Rassat, A., Starck, J.-L., & Dupe, F.-X. 2013, *A&A*, 557, A32
- Rassat, A., Starck, J.-L., Paykari, P., Sureau, F., & Bobin, J. 2014, *JCAP*, 8, 6
- Sachs, R. K. & Wolfe, A. M. 1967, *Astrophys. J.*, 147, 73
- Tegmark, M., Taylor, A. N., & Heavens, A. F. 1997, *ApJ*, 480, 22